Atomically Precise Arrays of Fluorescent Silver Clusters: A Modular Approach for Metal Cluster Photonics on DNA Nanostructures

Stacy M. Copp,[†] Danielle E. Schultz,[‡] Steven Swasey,[‡] and Elisabeth G. Gwinn*[,†]

[†]Department of Physics, University of California, Santa Barbara, California 93106-9530, United States and [‡]Department of Chemistry, University of California, Santa Barbara, California 93106-9510, United States

ABSTRACT The remarkable precision that DNA scaffolds provide for arraying nanoscale optical elements enables optical phenomena that arise from interactions of metal nanoparticles, dye molecules, and quantum dots placed at nanoscale separations. However, control of ensemble optical properties has been limited by the difficulty of achieving uniform particle sizes and shapes. Ligand-stabilized metal clusters offer a route to atomically precise arrays that combine desirable attributes of both metals and molecules. Exploiting the unique advantages of the cluster regime requires techniques to realize controlled nanoscale placement of select cluster structures. Here we show that atomically monodisperse arrays of fluorescent, DNA-stabilized silver clusters can be realized on a prototypical scaffold, a DNA nanotube, with attachment sites separated by <10 nm. Cluster attachment is mediated by designed DNA linkers that enable isolation of specific clusters prior to assembly on nanotubes and preserve cluster structure and spectral purity after assembly. The modularity of this approach generalizes to silver clusters of diverse sizes and DNA scaffolds of many types. Thus, these silver cluster nano-optical elements, which themselves have colors selected by their particular DNA templating oligomer, bring unique dimensions of control and flexibility to the rapidly expanding field of nano-optics.

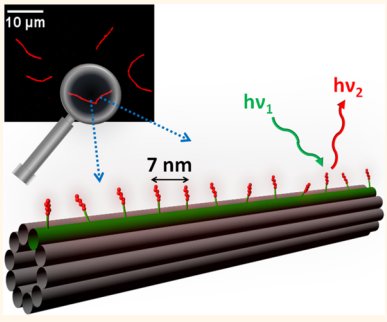

KEYWORDS: fluorescence · silver cluster · DNA nanotechnology · confocal microscopy · optical nanostructure · atomic precision

DNA nanotechnology enables nanoscale arrangement of optical elements, such as organic fluorophores, noble metal nanoparticles, and colloidal quantum dots, onto DNA scaffolds that self-assemble in diverse shapes and sizes.[1−6] Attachment of a single-stranded DNA oligomer (ssDNA) to a molecule or nanoparticle enables positioning at programed sites on DNA scaffolds by hybridization with complementary ssDNA extrusions on the scaffolds. Several groups have already employed hybridization to position optical elements on DNA nanostructures[4,5,7] and to demonstrate intriguing optical phenomena, including fluorescence resonance energy transfer (FRET),[8] optical chirality,[9,10] and surface-enhanced Raman scattering.[11]

Achieving desired optical properties from arrays of many elements demands stringent control over the individual elements. This is challenging for nanoparticles due to the difficulty of precisely controlling size, shape, and surface morphology.[12] In contrast, ligand-protected metal clusters provide a route to atomically precise control of size and shape[13] and, therefore, precise control over the optical response of cluster assemblies. Metal clusters are remarkable for their unique combination of metallic and molecular attributes, which can produce metal-like optical response from collective excitations of delocalized valence electrons while also exhibiting molecule-like high fluorescence quantum yields, related to the sparse density of states.[13−16] Crystallization of superlattices[17] composed of silver clusters protected by *p*-MBA ligands[18] was recently achieved. However, nanoscale arrangement of metal clusters by DNA-mediated methods, or by any other method achieving controlled nanoscale placement, is still an unrealized goal. Developing methods for arranging atomically precise metal clusters on the nanoscale is therefore a critical step toward

* Address correspondence to bgwinn@physics.ucsb.edu.

Received for review November 5, 2014 and accepted January 29, 2015.

Published online January 29, 2015
10.1021/nn506322q

harnessing their unique potential for applications in nanoscience.[19,20]

DNA-stabilized fluorescent silver clusters[21] (Ag_N-DNAs) are a new class of optical nanomaterial with unique advantages for arrangement on DNA scaffolds. Now employed in many applications,[22] Ag_N-DNAs are appealing for their tunable fluorescence colors, ranging from blue-green to near-IR,[23,24] high fluorescence quantum yields,[15] and proposed biocompatibility. Containing only $N \sim 10-30$ Ag atoms,[15] each silver cluster is stabilized by base motifs within a DNA template,[25] whose sequence selects the size of the cluster core and thus fluorescence color,[26] and whose linear arrangement, as constrained by the DNA backbone, imposes a unique, rod-like cluster shape.[15,26−28] This anisotropic shape is responsible for the wide color range of Ag_N-DNAs and for their strong polarization dependence,[15,29] which has fascinating potential for directionally dependent DNA-based optical materials.

These properties make Ag_N-DNAs uniquely suited for arrangement into atomically precise arrays on DNA scaffolds. While previous studies have used the preference for Ag cluster formation onto ssDNA to synthesize Ag_N-DNAs in linear arrays,[30,31] control of optical properties and spatial separations was not achieved due to the heterogeneous products formed during synthesis: typical templates give <10% chemical yields of a specific Ag_N-DNA, along with nonfluorescent majority products that have wide-ranging silver and DNA compositions.[15,32] Thus, in addition to the intended cluster, dark Ag products and Ag_N-DNA with the wrong fluorescence color decorate DNA scaffolds that are directly subject to Ag cluster synthesis. This heterogeneity of synthesis products is a nearly universal feature of Ag_N-DNAs that has been ignored in most prior studies.

Achieving atomically precise arrays of metal clusters requires a different approach. To realize decoration of DNA nanostructures with monodisperse silver clusters, we develop a modular, generalizable method to attach N atom silver clusters (Ag_N-DNA) onto individual selected double helices of 10-helix tiled DNA nanotubes (NT)[33] (Figure 1), chosen as prototypical scaffolds for linear arrays. We demonstrate this method with clusters of two sizes and distinct colors, $N = 15$ with 670 nm peak emission and $N = 14$ with 640 nm peak emission. We first describe design methods for the bifunctional DNA host strands that combine templates for fluorescent Ag_N-DNA with linker sequences, which both preserve cluster structure and hybridize to densely spaced attachment sites on NT. Next, NT attachment site design is presented. Confocal microscopy verifies NT decoration with Ag_N-DNA, and fluorescence spectroscopy verifies structural stability of Ag_N-DNA on NT.

RESULTS AND DISCUSSION

Ag_N-DNA Host Strand Design. We illustrate the design process for host strands for $N = 15$ clusters (Ag_{15});

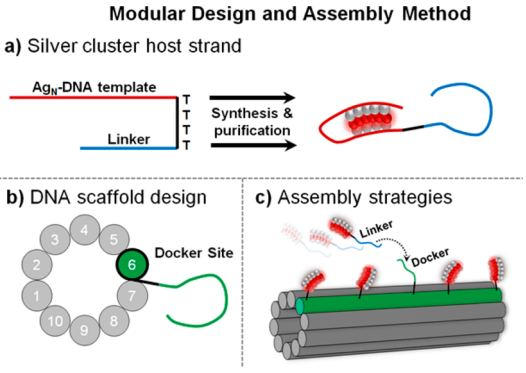

Figure 1. Attachment of monodiperse Ag_N-DNA to DNA nanotubes. Nanotubes (NT) self-assemble as 10 interwoven helices from 10 42-base strands reported previously,[33] with one strand extended here by a select 18-base "docker" sequence. (a) Modular cluster host strands constrain clusters to templating regions (red) with selection of noninteracting linker regions (blue). This allows Ag_N-DNA purification and, thus, selection of cluster size, N, prior to assembly on NT. (b) The docker (green), complementary to the linker, is appended to one of the strands that forms the NT and extrudes from the NT (end-view schematic). (c) NT decoration is mediated by Watson−Crick base pairing between diffusing linkers and extruding dockers that are spaced by 7.1 nm on the NT.

the same approach was successful for Ag_{14} (see Figure S3 and surrounding text). This Ag_{15}-DNA exhibits peak excitation and emission at 600 and 670 nm, respectively, and has a 75% fluorescence quantum yield.[15,34] The cluster's red emission results from a magic number of six neutral silver atoms in the cluster core.[26] Ag_{15}-DNA can be isolated by high-performance liquid chromatography (HPLC).[28] The DNA template sequence (Table S1, Supporting Information) was selected to produce this highly fluorescent, time-stable cluster, which is also robust at Mg^{2+} concentrations necessary for stable NT formation.

The bifunctional Ag_N-DNA host strand combines the cluster template sequence with an appended linker sequence. This linker attaches Ag_N-DNA to larger nanostructures that are decorated with complementary ssDNA "docker" sequences (Figure 1a). Using purification[32] prior to assembly, we recently showed that select Ag_N-DNA can be joined into simple dual-cluster assemblies with nanoscale separations using suitable complementary linkers.[34] "Suitable" linkers are essential: because the characteristics of base motifs for specific fluorescent clusters[25] are not well understood, intended linker sequences can disrupt the desired cluster structure when appended to the cluster template, causing altered color and/or loss of fluorescence.

Preservation of the structure of the selected Ag_N-DNA when the linker is present is established by preservation of the fluorescence spectrum, due to the strong correlation between emission wavelength and the elongated Ag_N cluster shape.[26,28] In addition to structure preservation, the linker must not form other silver products that would hinder hybridization to the

complementary docker, and insertion of dockers into the DNA nanostructure must not disrupt nanostructure formation. Finally, the complementary linker and docker must have a hybridization melting temperature sufficiently above room temperature but still be short enough to enable attachment of Ag_N-DNA at the high spatial densities that are a key advantage of DNA nanostructures.

Previously, DNA sequences rich in A and T were selected to link Ag_N-DNAs to other DNA strands because neither A nor T strongly associates with Ag_N.[34−37] These (A,T) linkers must be long, ∼ 30 bases, to achieve high-enough melting temperatures. We attempted to use a 30 base (A,T) sequence introduced by Yeh *et al.*[35,37] as a linker for Ag_{15}-DNA to NT. This was previously used to link Ag_{15}-DNA to a separate Ag_{10}-DNA, forming dilute solutions of dual-color cluster pairs exhibiting FRET.[34] However, the (A,T) sequence resulted in no detectable attachment of Ag_{15}-DNA and only very low attachment of linkers labeled with Cy5 to NT (Figure S1, Supporting Information). The failure of these long (A,T) linkers in the dense DNA environment on NT likely arises from a combination of steric crowding and partial linker self-complementarity caused by using only two base types.

For successful NT decoration, bifunctional host strands evidently require shorter, mixed-base linkers. Designing such a linker is challenged by the propensity of C and G to participate in templating Ag_N: appending these bases to a cluster template can change the species of Ag_N-DNA that forms. We evaluated several 10-base candidate linkers chosen from a set of 684 ssDNA strands with random (A,C,G,T) sequences, described elsewhere.[25,26] Selected linker candidates were chosen because they did not stabilize fluorescent Ag_N-DNA and had melting temperatures >40 °C with perfect complements (determined by UNAFold[38,39] for relevant salt concentrations). Candidate linkers were appended to the 3′ end of the Ag_{15}-DNA template. Comparison of the fluorescence spectra of unpurified Ag_N-DNA solutions, stabilized by the candidate host template-linker strands, to the spectrum with the template strand alone (Figure S2, Supporting Information) indicates that all linkers were successful; *i.e.*, Ag_{15} was the major fluorescent product in all cases. We selected the linker TCCGTTGTAT to use for attachment of the purified silver cluster to NT. Four additional A,T bases were appended to reach a linker-docker melting temperature >45 °C, and four thymine bases were inserted between template and linker. The final Ag_{15}-DNA host strand is then "template"-TTTT-TCCGTTGTATAAAT. After one round of HPLC purification using triethylamine acetate as the ion-pairing agent, peak emission wavelengths produced by the template alone and by the template-linker host strand agree within 1 nm, suggesting that the structure of the Ag_{15}-DNA is unperturbed by the linker.

We performed a second round of HPLC with in-line electrospray mass spectrometry (ESI-MS) in negative-ion mode to confirm that addition of this tail to the Ag_{15}-DNA template does not alter the composition of the fluorescent silver cluster (details in Methods). The second HPLC round used 1,1,1,3,3,3 hexafluoro-2-propanol/triethylamine as the ion-pairing agent to ensure sufficient ionization rates for high sensitivity MS.[32] MS confirms that the cluster stabilized by the modified Ag_{15}-DNA host strand contains 15 silver atoms (Figure S4, Supporting Information). The eluting Ag_{15}-DNA is estimated to be ≥70 ± 1% pure. HPLC−MS also confirms that the size of the Ag_{14}-DNA remains unchanged after addition of a tail and is isolated to 77.0 ± 0.1% purity (Figure S5, Supporting Information).

DNA Scaffold Design. We selected 10-helix DNA nanotubes[33] (NT) as scaffolds for Ag_N-DNA for two reasons: their architecture allows ssDNA docker extrusions at separations of just 7.1 nm along specific individual double helices of the NT, so that decorating elements are arrayed in a line (Figure 1), and their ∼10 μm length allows facile visiualization by fluorescence microscopy. To adapt published NT sequences[33] for decoration with Ag_N, we appended "docker" sequences (complementary to the linkers) to the end of one of the ten, 42-base oligomers that weave together to form the NT. A similar approach was previously taken to attach much larger colloidal gold nanoparticles to NT.[40] The ten NT strands offer 20 distinct docker sites. For Ag_{15}-DNA attachment, we chose to append the docker sequence to the 3′ end of strand U6, separated by TTTT to avoid perturbing the NT structure (see Table S1, Supporting Information, for nomenclature and sequences). Ag_{14}-DNA was attached to a U9-appended docker (details in the Supporting Information). To verify NT formation with docker strands, we used a fluorescein (FAM) dye label at the end of a different NT strand (U1) and imaged by confocal microscopy. Figures S6 and S7 (Supporting Information) show properly formed FAM-labeled NT.

Labeling Efficiency Control Experiments. FAM-labeled NT are models for 100% labeling with fluorescent elements spaced at 7.1 nm because FAM-labeling by the manufacturer is nearly 100% efficient and because the FAM-labeled U1 strand is necessary for NT assembly. Intensity profiles of NT decorated with Ag_N-DNA can therefore be compared to FAM-NT to investigate efficiency of docker site labeling by Ag_N-DNA. This comparison is necessary because previous studies of similar Cy3-labeled NT measured unexpected intensity modulations along NT contours.[40,41] Such modulations along the 100%-labeled Cy3-NT were attributed to deformations of NT structure caused by the strand extensions added to attach the dye labels. While such deformations do not alter the packing density of Cy3 dyes along the NT, they do modulate the coupling of

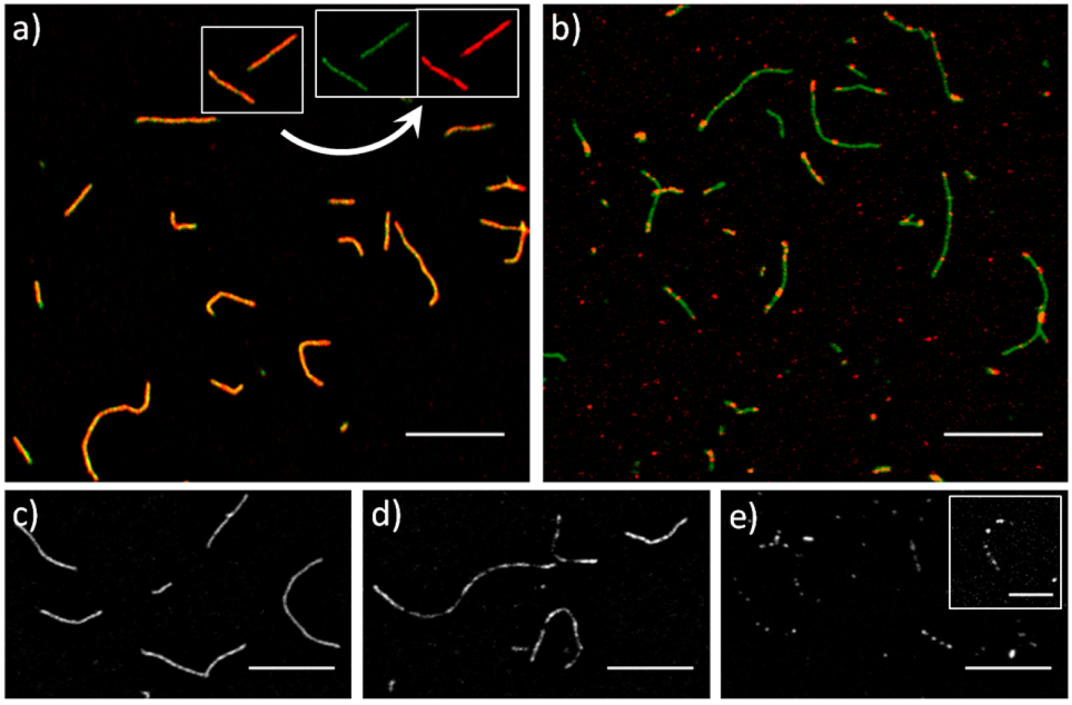

Figure 2. Fluorescence microscopy of NT decorated by Ag_{15}-DNA. (a–d) Spinning disk confocal images of 10-helix DNA nanotubes (NT) labeled with Ag_{15}-DNA and spin-cast in poly(vinyl alcohol) (PVA) film. Scale bars: 10 μm (except inset). (a, b) NT with FAM-labeled U1 strands and with (a) 100% of U6 strands with dockers and twice-purified Ag_{15}-DNA or (b) 10% of U6 with dockers and once-purified Ag_{15}-DNA. Yellow color indicates overlap of green (FAM) and red (Ag_{15}-DNA) fluorescence and, thus, attachment of Ag_{15}-DNA on NT. Inset in (a): FAM and Ag_{15}-DNA channels for boxed region. (c–e) Images of once-purified Ag_{15} (red) fluorescence only, with no FAM label. The percentage of U6 strands containing dockers controls the density of NT labeling by Ag_{15}-DNA: (c) 100% U6 dockers; (d) 50% U6 dockers; (e) widefield image of Ag_{15}-DNA on NT with 10% dockers shows more sparsely decorated NT. Inset: Confocal image of NT with 10% dockers, decorated by Ag_{15}-DNA. Inset scale bar: 5 μm.

emitted light into the microscope objective, causing the intensity modulations. Because we used the same strand extension modification (addition of two T bases, a dye linker, and a dye molecule to one end of a NT-forming oligomer) to label U1 strands with FAM, we expect, and observe, such intensity modulations. We also expect similar deformations of the NT decorated by Ag_N-DNA, due to the docker strand extensions.

To avoid confusing intensity modulations caused by such geometric deformations with regions of lower Ag_N-DNA labeling efficiency, we develop a numerical procedure to quantify intensity modulations along FAM-labeled NT and Ag_N-DNA-labeled NT. We used MATLAB-based software[42] to trace individual NT contours in confocal microscopy images. A custom MATLAB script, inspired by previous work,[41] then calculates the average standard deviation of the background-corrected intensity along each contour, normalized to the contour's average intensity, denoted by M (see Figure S8, Supporting Information, and surrounding text). M is a measure of the size of intensity fluctuations along a NT and thus correlates to average labeling efficiency. The most probable value of M is ~0.2 for FAM-NT (Figure 3).

M values for FAM-NT are larger than expected if the orientation of the dye-labeled helix does not vary along an NT (see simulations, Figure S9, Supporting Information). The microscope point spread function brings ~30 FAM molecules, spaced 7.1 nm apart, within a diffraction limited spot. Thus, $M \sim 0$ if emitted light collection is uniform along NT and if emission dipole directions randomize during the collection time. Assuming random, fixed dipole orientations raises the expected M to ~0.1 (Figure S9, Supporting Information), still below the most probable observed $M \sim 0.2$ (Figure 3). Apparently the strand extensions protruding from the NT do perturb its shape, as previously observed.[40,41]

Microscopy of NT Decorated by Ag_N-DNA. Assembly of NT decorated with Ag_N-DNA demonstrates the modularity of our method. First, Ag_N are synthesized on a cluster host strand, which combines the cluster template sequence with a linker sequence. Silver clusters with a particular size, N, are then isolated, removing dark cluster products that would otherwise occupy NT sites. Next, NT-forming DNA strands, with docker sites attached to one of these strands, are annealed by heating to 90 °C and then cooling over 25 h from 65 to 50 °C, across the NT melting transition. Decoration of NT with select Ag_N-DNA (N = 14 or 15) is then simply mediated by the designed linker and docker regions, whose >45 °C melting temperature allows room temperature assembly (full assembly details in Methods). Confocal microscopy confirms decoration of NT with

Ag_{15}-DNA (Figure 2; Ag_{14}-DNA decoration in Figure S10, Supporting Information). NT in Figure 2a, b are colabeled with FAM, and colocalized fluorescence from FAM (green) and Ag_{15}-DNA (red) confirms Ag_{15}-DNA attachment. No Ag_{15}-DNA attachment is observed for NT without docker sites (data not shown). Parts c−e of Figure 2 shows that the density of dockers on the NT controls Ag_N-DNA labeling density, confirming that Ag_{15}-DNA attach by hybridization of linkers and dockers. For NT with dockers appended to 100% of the U6 strands, NT appear continuously labeled by fluorescent clusters (Figure 2c). In comparison, coverage is less uniform for dockers on just 50% of the U6 docker sites, with some micron-scale variations in intensity along the NT (Figure 2d). NT with 10% U6 docker sites are sparsely decorated (Figure 2b,e), and individual Ag_{15}-DNA emitters can be identified by stepwise blinking and bleaching (movie S1, Figure S11, Supporting Information).

Labeling Efficiency. To investigate the labeling efficiency of NT by Ag_{15}-DNA, we compared intensity modulations along NT with 100% U6 dockers that were decorated by Ag_{15}-DNA (Figure 2a,c) to FAM-labeled NT with both 100% U6 dockers and FAM-labeled U1 (Figure S6, Supporting Information), using the previously described numerical measure *M*. The probability density functions (PDFs) of *M* for 100% labeled FAM-NT (green) and NT, with 100% U6 dockers, labeled by twice-purified Ag_{15}-DNA (red) show close similarity (Figure 3). Because FAM-NT are models for 100% labeled NT, this similarity suggests that average NT labeling efficiency with Ag_{15}-DNA is also near 100%.

Ag_N-DNA Spectroscopy. In addition to NT deformations caused by decorating elements and/or docker site extrusions, NT may also deform the structures of the decorating Ag_N-DNAs themselves. It is well-known that an Ag_N-DNA's optical properties can be extremely sensitive to the local cluster environment, a feature that is the basis for a number of fascinating sensing applications.[22,35,37] Thus, it is important to investigate whether the proximity of Ag_N-DNA to much larger NT DNA scaffolds affects the structure of the decorating clusters. Possible structural reconfigurations include changes in the number of neutral Ag atoms, which correlates strongly with color, and changes in the number of Ag cations, which may have finer control of Ag_N-DNA shape.[26] The proximity of Ag_N-DNA to NT containing orders of magnitude more DNA than the cluster host strands, may also affect cluster geometry and/or radiative properties. To investigate whether Ag_N-DNA properties are changed by attachment to NT scaffolds, we compared fluorescence spectroscopy for Ag_N-DNA free in solution to Ag_N-DNA attached to NT with 100% docker sites. UV excitation was used to universally excite all Ag_N-DNA products simultaneously.[43]

The UV-excited fluorescence spectra of Ag_{14}-DNA and Ag_{15}-DNA (Figure 4) have unshifted emission peaks and unaltered peak widths when bound to docker sites (red) on NT as compared to free in solution (black). Because the fluorescence spectrum of an Ag_N-DNA is highly sensitive to changes in cluster geometry,[26,28] such unchanged spectral shapes indicate that these Ag_N-DNA are unaltered by scaffolding on NT.

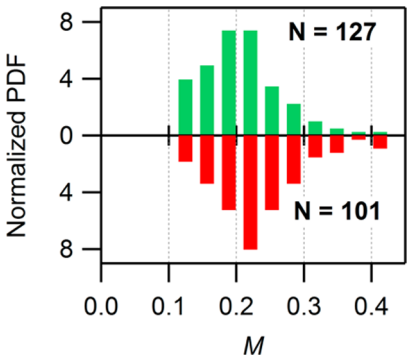

Figure 3. Intensity fluctuations along NT. Normalized probability density functions (PDFs) for *M*, the average standard deviation of the background-corrected intensity, normalized to average intensity, along *N* individual NT contours. Top (green): FAM-NT, with 100% U6 docker sites and 100% U1-FAM, are a model for 100% labeling. Intensity variations that arise from NT deformations modulate the coupling of emitter dipoles in the objective, resulting in nonzero measured values of *M*. Bottom (red): The same NT with 100% U6 dockers decorated by twice-purified Ag_{15}−DNA. Similar PDFs suggest that percent labeling with Ag_{15} is similar to that for 100% FAM (7 nm spacing).

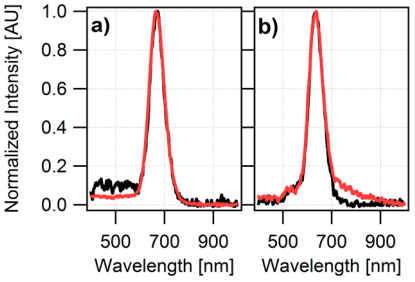

Figure 4. Ag_N-DNA emission on and off NT. UV-excited fluorescence spectra of (a) Ag_{15}-DNA and (b) Ag_{14}-DNA free in solution (black) and attached to NT (red). (a) Ag_{15}-DNA mixed with 5× excess of NT containing 100% U6 docker sites to ensure complete Ag_{15}-DNA binding, and incubated at room temperature for 75 min (red) show unchanged spectral features compared to Ag_{15}-DNA at identical concentrations and incubation times but in the absence of NT (black). (b) Ag_{14}-DNA, mixed at 5× excess of NT with U9 docker sites (red) maintain a dominant 640 nm peak, the same as Ag_{14}-DNA free in solution (black).

CONCLUSIONS

In conclusion, we have demonstrated a modular design and assembly method for decorating DNA nanotube structures with atomically precise arrays of fluorescent silver clusters. Bifunctional host strands constrain the cluster to a templating region of the strand, while a separate linker region allows attachment to ssDNA "docker" extrusions from a prototypical

scaffold, a DNA nanotube, after the crucial step of isolating a particular cluster species. Positioning of individual Ag_N-DNA of known size, *N*, at selected locations on the nanotubes *via* ssDNA docker sites, is verified using fluorescence microscopy. Fluorescence spectroscopy shows that the optical properties of these Ag_N-DNA, and thus cluster structure, are unaffected by proximity to the DNA nanostructure. This modular approach to scaffold decoration with Ag_N of select size, *N*, represents the first demonstration of nanoscale assembly of atomically precise metal clusters at programmed positions on a nanoscale scaffold. The approach should generalize across a diverse spectrum of DNA scaffold sizes and geometries as well as to patterned scaffolding of silver clusters with different *N* and different emission colors.

METHODS

Ag_N-DNA Synthesis, Purification, And Characterization. DNA templates for Ag_N-DNA were ordered from Integrated DNA Nanotechnologies (IDT) with standard desalting. Template DNA was mixed with $AgNO_3$ in a 10 mM NH_4OAc ammonium acetate buffer and incubated at room temperature for 20 min. DNA–silver solutions were then reduced using $NaBH_4$ and mixed well. Final concentrations for synthesizing Ag_{15}-DNA and Ag_{14}-DNA were 15.0 μM DNA, 188 μM $AgNO_3$, and 93.8 μM $NaBH_4$ (corresponding to 12.5 Ag atoms per host strand; Ag/base ratios vary with host strand length). Ag_{14}-DNA purified by HPLC was synthesized using 25 μM DNA, 313 μM $AgNO_3$, and 156 μM $NaBH_4$ (12.5 Ag atoms per host strand). Samples were stored at 4 °C overnight prior to spectral characterization and/or purification using reverse-phase high-performance liquid chromatography (HPLC). Emission spectra were collected with a thermoelectrically cooled array detector (Ocean Optics QE65000) and SpectraSuite software (Ocean Optics). A UV LED was used to universally excite fluorescence of Ag_N-DNA.[43]

A 2695 Separations Module with autoinjector and 2487 Dual Wavelength absorbance detector (10 μL volume), set to monitor the visible peak of each silver cluster, were used to perform HPLC (Waters). Full emission spectra were also collected every second by the Ocean Optics QE65000, using the UV LED to universally excite all Ag_N-DNA products. A first separation of different Ag_N-DNA species was achieved using linear gradients of H_2O and MeOH in the ion-pairing agent, 35 mM triethylamine acetate (TEAA), to a 50 mm × 4.6 mm Kinetex C18 core–shell column (Phenomenex). The second round of purification, by the same instrument and column but in-line with the MS, used running buffers with 400 mM 1,1,1,3,3,3-hexafluoro-2-propanol in separate H_2O and MeOH solutions adjusted to pH 7 with triethylamine. Samples were purified using a 1% per minute linear gradient of 15–35% methanol running buffer. Ag_N-DNA were returned to 10 mM NH_4OAc by spin filtration with Amicon Ultra 3 kDa membrane centrifugal filters (EMD Millipore).

Mass spectra were collected every 1 s over a 500–3000 *m/z* range on a Waters QTOF2 in electrospray ionization negative mode. Instrument parameters were set to 2 kV capillary voltage, 30 V cone voltage, 10 V collision energy, 100 °C source, and 120 °C desolvation temperatures. Samples were introduced into the MS at 10 μL/min through a splitter connected to the HPLC, allowing simultaneous collection and characterization.

DNA Nanotube Assembly. Ten-helix DNA nanotubes[33] (NT) were formed with HPLC-purified oligomers from IDT (sequences provided in Table S1, Supporting Information). For fluorescein-labeled NT, U1 oligomers were ordered from IDT with a fluorescein dye (FAM) attached to the 5′ end. The 10 NT-forming oligomers were mixed in 0.2 mL PCR tubes, each oligomer at a final concentration of 1.4 μM, in 40 mM NH_4OAc and 12 mM MgOAc for a final volume of 50 μL. Mixtures were annealed using a Mastercycler personal (Eppendorf) to heat solutions to 90 °C for 5 min and then cool solutions from 65 to 50 °C in 0.5 °C steps, 50 min per step. After annealing, NT were stored at 4 °C for no more than several days until use. For NT with varying % dockers, U6 and U6-docker site oligomers were mixed at appropriate ratios for a total final concentration of [U6 + U6-linker] = 1.4 μM.

Decoration of NT with Ag_N-DNA. To attach Ag_N-DNA to NT, Ag_N-DNA was added to solutions of annealed NT, at 5 times greater Ag_N-DNA concentration than the concentration of docker sites appended to NT, for final NT concentration of 0.14 μM and a final Ag_N-DNA concentration of 5 × (% docker) × 0.14 μM. For NT decorated with twice-purified Ag_{15}-DNA, final NT and Ag_{15}-DNA concentrations were halved to conserve material. Buffer concentration was maintained at 40 mM NH_4OAc and 12 mM MgOAc after mixing. Mixtures were stored for at least 1 h at room temperature in the dark before imaging.

Microscopy. Standard microscopy coverslips (#1.5) were sequentially sonicated for 15 min in acetone, ethanol, and 18.2 MΩ·cm H_2O (Milli-Q, Millipore) and then dried in an oven. Glass slides were rinsed well in 18.2 MΩ·cm H_2O and then ethanol and subsequently dried under filtered N_2. For samples embedded in polyvinyl alchohol (PVA), 16 kDa PVA (Acros Organics) was dissolved in H_2O at 5 mg/mL. NT-Ag_N-DNA mixture (1 μL) was added to 90 μL of PVA and 9 μL of H_2O and immediately spun-cast on clean coverslips at 1680 rpm for 100 s. Coverslips were fixed above the microscope objective on a clean glass slide. Widefield and confocal fluorescence microscopy were performed using an inverted Olympus DSU (Spinning Disk) confocal with a Hamamatsu ImaEM CCD camera (C9100-13) and Hg arc lamp illumination. A 89000 ET Sedat Quad Filter Set (Chroma) was used to image fluorescein-labeled NT and Ag_{14}-DNA, and a Cy5-4040A filter set was used for imaging Ag_{15}-DNA (Semrock). A UPlanSApo 100X oil immersion objective, with 1.4 numerical aperture (NA) (Olympus), was used to collect all images, with standard acquisition times of 1 s. For widefield images of NT with 10% docker sites (Figure 2e, not including inset), the spinning disk was removed to increase collected fluorescence signal. Confocal images of NT with 10% docker sites were collected with 10–15 s exposure times. MetaMorph software was used to control image acquisition (Molecular Devices, Inc.).

Conflict of Interest: The authors declare no competing financial interest.

Acknowledgment. We dedicate this paper in memory of those students who lost their lives in the Isla Vista tragedy and to the courage of the first responders, whose selfless actions saved many lives. This work was supported by NSF-CHE-1213895. We thank Alexis Faris and Jacqueline Geler-Kremer for preliminary fluorescence studies, Dr. Mary Raven for training and assistance with microscopy, Dirk Bouwmeester and Nemanja Markešević for discussions of microscopy, and Deborah Fygenson and Daniel Schiffels for discussions about DNA NT. We acknowledge the use of the NRI-MCDB Microscopy Facility at UC Santa Barbara. S.M.C. acknowledges support from NSF-DGE-1144085 (NSF Fellowship).

Supporting Information Available: DNA sequences for Ag_N-DNA host strands and nanotube oligomers, design details for Ag_{14}-DNA host strand, HPLC-MS data, additional microscopy images, movie of single Ag_{15}-DNA blinking, nanotube contour tracing details, and nanotube contour simulations. This material is available free of charge *via* the Internet at http://pubs.acs.org.

REFERENCES AND NOTES

1. Winfree, E.; Liu, F.; Wenzler, L. A.; Seeman, N. C. Design and Self-Assembly of Two-Dimensional DNA Crystals. *Nature* **1998**, *394*, 539–544.

2. Rothemund, P. W. K. Folding DNA to Create Nanoscale Shapes and Patterns. *Nature* **2006**, *440*, 297–302.
3. Douglas, S. M.; Dietz, H.; Liedl, T.; Högberg, B.; Graf, F.; Shih, W. M. Self-Assembly of DNA into Nanoscale Three-Dimensional Shapes. *Nature* **2009**, *459*, 414–418.
4. Zheng, J.; Constantinou, P. E.; Micheel, C.; Alivisatos, A. P.; Kiehl, R. A.; Seeman, N. C. Two-Dimensional Nanoparticle Arrays Show the Organizational Power of Robust DNA Motifs. *Nano Lett.* **2006**, *6*, 1502–1504.
5. Schreiber, R.; Do, J.; Roller, E.-M.; Zhang, T.; Schüller, V. J.; Nickels, P. C.; Feldmann, J.; Liedl, T. Hierarchical Assembly of Metal Nanoparticles, Quantum Dots and Organic Dyes Using DNA Origami Scaffolds. *Nat. Nanotechnol.* **2014**, *9*, 74–78.
6. Ko, S. H.; Du, K.; Liddle, J. A. Quantum-Dot Fluorescence Lifetime Engineering with DNA Origami Constructs. *Angew. Chem., Int. Ed.* **2013**, *52*, 1193–1197.
7. Ding, B.; Deng, Z.; Yan, H.; Cabrini, S.; Zuckermann, R. N.; Bokor, J. Gold Nanoparticle Self-Similar Chain Structure Organized by DNA Origami. *J. Am. Chem. Soc.* **2010**, *132*, 3248–3249.
8. Stein, I. H.; Schüller, V.; Böhm, P.; Tinnefeld, P.; Liedl, T. Single-Molecule FRET Ruler Based on Rigid DNA Origami Blocks. *ChemPhysChem* **2011**, *12*, 689–695.
9. Kuzyk, A.; Schreiber, R.; Fan, Z.; Pardatscher, G.; Roller, E.-M.; Högele, A.; Simmel, F. C.; Govorov, A. O.; Liedl, T. DNA-Based Self-Assembly of Chiral Plasmonic Nanostructures with Tailored Optical Response. *Nature* **2012**, *483*, 311–314.
10. Shen, X.; Asenjo-Garcia, A.; Liu, Q.; Jiang, Q.; García de Abajo, F. J.; Liu, N.; Ding, B. Three-Dimensional Plasmonic Chiral Tetramers Assembled by DNA Origami. *Nano Lett.* **2013**, *13*, 2128–2133.
11. Pilo-Pais, M.; Watson, A.; Demers, S.; LaBean, T. H.; Finkelstein, G. Surface-Enhanced Raman Scattering Plasmonic Enhancement Using DNA Origami-Based Complex Metallic Nanostructures. *Nano Lett.* **2014**, *14*, 2099–2104.
12. Lee, Y.-J.; Schade, N. B.; Sun, L.; Fan, J. A.; Bae, D. R.; Mariscal, M. M.Lee, G.; Capasso, F.; Sacanna, S.; Manoharan, V. N.; et al. Ultrasmooth, Highly Spherical Monocrystalline Gold Particles for Precision Plasmonics. *ACS Nano* **2013**, *7*, 11064–11070.
13. Häkkinen, H. Atomic and Electronic Structure of Gold Clusters: Understanding Flakes, Cages and Superatoms from Simple Concepts. *Chem. Soc. Rev.* **2008**, *37*, 1847–1859.
14. Guidez, E. B.; Aikens, C. M. Diameter Dependence of the Excitation Spectra of Silver and Gold Nanorods. *J. Phys. Chem. C* **2013**, *117*, 12325–12336.
15. Schultz, D.; Gardner, K.; Oemrawsingh, S. S. R.; Markešević, N. Olsson, K.; Debord, M.; Bouwmeester, D.; Gwinn, E. Evidence for Rod-Shaped DNA-Stabilized Silver Nanocluster Emitters. *Adv. Mater.* **2013**, *25*, 2797–2803.
16. Yu, Y.; Luo, Z.; Chevrier, D. M.; Leong, D. T.; Zhang, P.; Jiang, D.; Xie, J. Identification of a Highly Luminescent $Au_{22}(SG)_{18}$ Nanocluster. *J. Am. Chem. Soc.* **2014**, *136*, 1246–1249.
17. Yoon, B.; Luedtke, W. D.; Barnett, R. N.; Gao, J.; Desireddy, A.; Conn, B. E.; Bigioni, T.; Landman, U. Hydrogen-Bonded Structure and Mechanical Chiral Response of a Silver Nanoparticle Superlattice. *Nat. Mater.* **2014**, *13*, 807–811.
18. Desireddy, A.; Conn, B. E.; Guo, J.; Yoon, B.; Barnett, R. N.; Monahan, B. M.; Kirschbaum, K.; Griffith, W. P.; Whetten, R. L.; Landman, U.; et al. Ultrastable Silver Nanoparticles. *Nature* **2013**, *501*, 399–402.
19. Niihori, Y.; Matsuzaki, M.; Pradeep, T.; Negishi, Y. Separation of Precise Compositions of Noble Metal Clusters Protected with Mixed Ligands. *J. Am. Chem. Soc.* **2013**, *135*, 4946–4949.
20. Xu, L.; Ma, W.; Wang, L.; Xu, C.; Kuang, H.; Kotov, N. A. Nanoparticle Assemblies: Dimensional Transformation of Nanomaterials and Scalability. *Chem. Soc. Rev.* **2013**, *42*, 3114–3126.
21. Petty, J. T.; Zheng, J.; Hud, N. V.; Dickson, R. M. DNA-Templated Ag Nanocluster Formation. *J. Am. Chem. Soc.* **2004**, *126*, 5207–5212.
22. Yuan, Z.; Chen, Y.-C.; Li, H.-W.; Chang, H.-T. Fluorescent Silver Nanoclusters Stabilized by DNA Scaffolds. *Chem. Commun. (Camb).* **2014**, *50*, 9800–9815.
23. Gwinn, E. G.; O'Neill, P.; Guerrero, A. J.; Bouwmeester, D.; Fygenson, D. K. Sequence-Dependent Fluorescence of DNA-Hosted Silver Nanoclusters. *Adv. Mater.* **2008**, *20*, 279–283.
24. Petty, J. T.; Fan, C.; Story, S. P.; Sengupta, B.; Sartin, M.; Hsiang, J.-C.; Perry, J. W.; Dickson, R. M. Optically Enhanced, near-IR, Silver Cluster Emission Altered by Single Base Changes in the DNA Template. *J. Phys. Chem. B* **2011**, *115*, 7996–8003.
25. Copp, S. M.; Bogdanov, P.; Debord, M.; Singh, A.; Gwinn, E. Base Motif Recognition and Design of DNA Templates for Fluorescent Silver Clusters by Machine Learning. *Adv. Mater.* **2014**, *26*, 5839–5845.
26. Copp, S. M.; Schultz, D.; Swasey, S.; Pavlovich, J.; Debord, M.; Chiu, A.; Olsson, K.; Gwinn, E. Magic Numbers in DNA-Stabilized Fluorescent Silver Clusters Lead to Magic Colors. *J. Phys. Chem. Lett.* **2014**, *5*, 959–963.
27. Ramazanov, R. R.; Kononov, A. I. Excitation Spectra Argue for Threadlike Shape of DNA-Stabilized Silver Fluorescent Clusters. *J. Phys. Chem. C* **2013**, *117*, 18681–18687.
28. Swasey, S. M.; Karimova, N.; Aikens, C. M.; Schultz, D. E.; Simon, A. J.; Gwinn, E. G. Chiral Electronic Transitions in Fluorescent Silver Clusters Stabilized by DNA. *ACS Nano* **2014**, *8*, 6883–6892.
29. Markešević, N.; Oemrawsingh, S. S. R.; Schultz, D.; Gwinn, E. G.; Bouwmeester, D. Polarization Resolved Measurements of Individual DNA-Stabilized Silver Clusters. *Adv. Opt. Mater.* **2014**, *2*, 765–770.
30. O'Neill, P. R.; Young, K.; Schiffels, D.; Fygenson, D. K. Few-Atom Fluorescent Silver Clusters Assemble at Programmed Sites on DNA Nanotubes. *Nano Lett.* **2012**, *12*, 5464–5469.
31. Orbach, R.; Guo, W.; Wang, F.; Lioubashevski, O.; Willner, I. Self-Assembly of Luminescent Ag Nanocluster-Functionalized Nanowires. *Langmuir* **2013**, *29*, 13066–13071.
32. Schultz, D.; Gwinn, E. G. Silver Atom and Strand Numbers in Fluorescent and Dark Ag:DNAs. *Chem. Commun. (Cambridge)* **2012**, *48*, 5748–5750.
33. Yin, P.; Hariadi, R. F.; Sahu, S.; Choi, H. M. T.; Park, S. H.; Labean, T. H.; Reif, J. H. Programming DNA Tube Circumferences. *Science* **2008**, *321*, 824–826.
34. Schultz, D.; Copp, S. M.; Markešević, N.; Gardner, K.; Oemrawsingh, S. S. R.; Bouwmeester, D.; Gwinn, E. Dual-Color Nanoscale Assemblies of Structurally Stable, Few-Atom Silver Clusters, as Reported by Fluorescence Resonance Energy Transfer. *ACS Nano* **2013**, *7*, 9798–9807.
35. Yeh, H.-C.; Sharma, J.; Shih, I.-M.; Vu, D. M.; Martinez, J. S.; Werner, J. H. A Fluorescence Light-up Ag Nanocluster Probe That Discriminates Single-Nucleotide Variants by Emission Color. *J. Am. Chem. Soc.* **2012**, *134*, 11550–11558.
36. Schultz, D.; Gwinn, E. Stabilization of Fluorescent Silver Clusters by RNA Homopolymers and Their DNA Analogs: C,G *versus* A,T(U) Dichotomy. *Chem. Commun. (Camb).* **2011**, *47*, 4715–4717.
37. Yeh, H.-C.; Sharma, J.; Han, J. J.; Martinez, J. S.; Werner, J. H. A DNA--Silver Nanocluster Probe That Fluoresces upon Hybridization. *Nano Lett.* **2010**, *10*, 3106–3110.
38. Markham, N. R.; Zuker, M. DINAMelt Web Server for Nucleic Acid Melting Prediction. *Nucleic Acids Res.* **2005**, *33*, W577–W581.
39. Markham, N. R.; Zuker, M. UNAFold: Software for Nucleic Acid Folding and Hybridization. In *Bioinformatics, Vol. II: Structure, Function, and Applications*; Keith, J. M., Ed.; Methods in Molecular Biology; Humana Press: Totowa, NJ, 2008; Vol. 453, pp 3–31.
40. Schiffels, D.; Liedl, T.; Fygenson, D. K. Nanoscale Structure and Microscale Stiffness of DNA Nanotubes. *ACS Nano* **2013**, *7*, 6700–6710.
41. Schiffels, D. *Design, Characterization and Functionalization of DNA Materials*; Ludwig-Maximilians-Universität: München, 2013.

42. Wiggins, P. A.; van der Heijden, T.; Moreno-Herrero, F.; Spakowitz, A.; Phillips, R.; Widom, J.; Dekker, C.; Nelson, P. C. High Flexibility of DNA on Short Length Scales Probed by Atomic Force Microscopy. *Nat. Nanotechnol.* **2006**, *1*, 137–141.
43. O'Neill, P. R.; Gwinn, E. G.; Fygenson, D. K. UV Excitation of DNA Stabilized Ag Cluster Fluorescence *via* the DNA Bases. *J. Phys. Chem. C* **2011**, *115*, 24061–24066.